

National Central University

國立中央大學

Department of Atmospheric Science

College of Earth Science

大氣科學學系

地球科學學院

Doctoral Dissertation

博士論文

Urban impacts on tropospheric ozone chemistry and
ozone abatement strategy using a CMAQ-PMF-based
composite index

使用基於 CMAQ-PMF 的綜合指數探討對流層臭氧化
學對都市的影響及臭氧減少策略

Author (研究生): Jackson Chang Hian Wui (鄭顯威)

Thesis Advisor (指導教授): Professor Neng-Huei Lin (林能暉教授)

Dec 2022

中華民國 111 年 12 月

National Central University Library Authorization for Thesis/ Dissertation

Application Date: 2022/12/30

The latest version since Sep. 2019

Applicant Name	Jackson Chang Hian Wui	Student Number	108681601
Schools / Departments	Department of Atmospheric Science	Graduate Degree	<input type="checkbox"/> Master <input checked="" type="checkbox"/> Doctor
Thesis/Dissertation Title	Urban impacts on tropospheric ozone chemistry and ozone abatement strategy using a CMAQ-PMF-based composite index	Advisor Name	Lin Neng-Huei

Authorization for Internet Access of Thesis/ Dissertation

This license authorizes my complete electronic thesis to be archived and read in the

• National Central University Library Electronic Theses & Dissertations System .

(X) Released for Internet access immediately

() Released for Internet access starting from: _____/_____/_____(YYYY / MM / DD)

() Disagree, because: _____

• NDLTD(National Digital Library of Theses and Dissertations in Taiwan).

() Released for Internet access immediately

() Released for Internet access starting from: _____/_____/_____(YYYY / MM / DD)

() Disagree, because: _____

I hereby agree to authorize the electronic versions of my thesis/dissertation and work to National Central University, University System of Taiwan(UST) and National Central Library(National Digital Library of Theses and Dissertations in Taiwan), in a non-exclusive way and without reimbursement, in accordance with the Copyright Act. The fore-mentioned authorized items can be reproduced by the authorized institution in the form of text, video tape, audio tape, disc and microfilm, or converted into other digital formats, without the limitation of time, places, and frequency for non-commercial uses.

Delayed Public Release for Paper Copy of Thesis/Dissertation

(You do not need to fill out this section if you make the paper copy of your thesis/dissertation available to the public immediately.)

• Reasons for the delayed release (choose one)

() Filing for patent registration. Registration number: _____

() Submission for publication

() Your research contains information pertaining to national non-disclosure agreements.

() Contents withheld according to the law. Please specify _____

• Delayed Until : _____/_____/_____(YYYY / MM / DD)

You should submit another paper copy to National Central Library (NCL) through the NCU Division of Registrar. If you would like to delay the release of this paper copy in NCL, please fill out the "Application for Embargo of thesis/dissertation" of NCL.

Signature of the Applicant: _____

Signature of the Advisor: _____

*Please attach this form after the thesis/dissertation cover when submitting your thesis/dissertation.

國立中央大學博士班研究生

論文指導教授推薦書

大氣科學 學系/研究所 鄭顯威 研

究生所提之論文 使用基於 CMAQ-PMF 的綜合
指數探討對流層臭氧化學對都市的影響及臭氧減
少策略係由本人指導撰述，同意提付審查。



指導教授  (簽章)

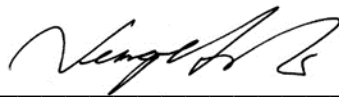
2022 年 12 月 30 日

National Central University

Advisor's Recommendation for Doctoral Students

This thesis is by Jackson Chang Hian Wui of the graduate program in Department of Atmospheric Science, entitled: Urban impacts on tropospheric ozone chemistry and ozone abatement strategy using a CMAQ-PMF-based composite index, which is written under my supervision, and I agree to propose it for examination.

Advisor



2022/12/30 (YYYY/MM/DD)

National Central University

Verification Letter from the Oral Examination Committee for Doctoral
Students

This thesis titled “Urban impacts on tropospheric ozone chemistry and ozone abatement strategy using a CMAQ-PMF-based composite index” studying in the graduate program in Department of Atmospheric Science. The author of this thesis is qualified for a Doctoral degree through the verification of the committee.

Convener of the Degree Examination Committee

Ming-Cheng Yen

Members

Hsin-chih Lai

Neap Shu

Guoy-Dong Shu

Ming Tung Chuang,

Sheng-Hong Wang

Date: 2022/12/30
(YYYY/MM/DD)

1080618

Abstract

Recent rapid urbanization has had a profound impact on local-scale atmospheric circulation but its impacts on the physical and chemical processes controlling the tropospheric ozone remain poorly resolved. In Taiwan, due to the strict emission policy, the ambient concentrations of nitrogen oxides (NO_x) and volatile organic compounds (VOCs) have reduced by nearly 60% since 1994. However, such reduction in precursors has not been linearly reflected on the annual mean ozone concentration, but an increasing or flattening trend is seen in the last decade. Therefore, a comprehensive investigation on the urban impacts on tropospheric ozone chemistry is necessary for prescribing an effective ozone abatement strategy. Our study area focuses on southern Taiwan, a complex region of coastal urban and industrial parks and inland mountainous areas, where high ozone episode often occurs during the seasonal transition period (i.e. Apr-May and Oct-Nov). In this thesis, we modelled the spatial and temporal distribution of ozone and its precursors (i.e. NO_x and VOCs) using WRF-CMAQ model at urban scale resolution 1.0×1.0 km.

Firstly, we investigated the impacts of urban land-surface forcing and its interaction with local circulations on local meteorology and ozone air quality. Two simulations were performed with the same emissions but different land cover designations: URBAN scenario represents the current urbanized condition and NO-URBAN scenario replaces all urban grid cells with cropland. It was shown that when the urban-heat-island (UHI) convergent flow stalls over the city, a circulation flow is formed and traps the pollutants at an elevated height, increasing the reaction of hydroxyl radical with VOCs by $2.0\text{-}4.0$ ppbv h^{-1} at $1000\text{-}1500$ m. At nighttime, the deeper boundary layer of URBAN scenario diluted NO_x mixing ratio by 17 ppbv and weakened the titration effect, causing higher O_3 concentration by 15 ppbv in the urban area. When the UHI vertical mixing diminished, the O_3 aloft diffused downward to the surface level and further degraded the nighttime air quality.

Secondly, we examined the budget analysis of boundary-layer O_3 , NO_x and NMHC over the urban and inland area of southern Taiwan. In the near-surface budget, chemical process and dry deposition are the main sink of O_3 with the contribution more than 10 ppbv h^{-1} and 15 ppbv h^{-1} , respectively; the major source of near-surface O_3 is vertical diffusion exceeding 30 ppbv h^{-1} . In the boundary-layer budget, chemical process is the main source while vertical diffusion becomes the sink for O_3 . The physiochemical circulation involves the vertical transport of near-surface pollutants and enhances photochemical production of O_3 in the upper PBL level is dominant in urban areas. This vertical exchange is mainly attributed to the vertical diffusion process and gradually decreases with heights. Our results highlighted the important role of daytime sea breeze circulation pushing the polluted urban air masses into the inland region which greatly

enhanced the inland O_3 production due to the NO_x -limited condition. Thus, control of NO_x emission in inland area may be ineffective due to the dynamics role of land-sea breeze; whereas most of the urban areas are characterized by VOC-limited condition where control of VOCs emission is helpful to reduce urban O_3 concentration.

Thirdly, we developed a CMAQ-PMF-based composite index to identify the key VOC source-species for effective ozone abatement strategy. First-order, second-order and cross sensitivities of ozone concentrations to domain-wide (i.e. urban, suburban and rural) NO_x and VOC emissions were determined for the study area using CMAQ-Higher Direct Decoupled Method (HDDM). Negative (positive) first-order sensitivities to NO_x emissions are dominant over urban (inland) areas, confirming ozone production sensitivity favors the VOC-limited regime (NO_x -limited regime) in southern Taiwan. Most of the urban areas exhibited negative second-order sensitivity to NO_x emissions, indicating a negative O_3 convex response where the linear increase of O_3 from decreasing NO_x emissions was largely attenuated by the non-linear effects. Due to the solidly VOC-limited regime and the relative insensitivity of O_3 production to increases or decreases of NO_x emissions, this study pursued the VOC species that contributed the most to ozone formation. PMF analysis driven by VOCs resolved 8 factors including mixed industry (21%), vehicle emissions (22%), solvent usage (17%), biogenic (12%), plastic industry (10%), aged air mass (7%), motorcycle exhausts (7%), and manufacturing industry (5%). Based on the CMAQ-PMF-based composite index, our results indicate that VOC control measures should prioritize (1) solvent usage for painting, coating and the printing industry, which emits abundant toluene and xylene, (2) gasoline fuel vehicle emissions of n-butane, isopentane, isobutane and n-pentane, and (3) ethylene and propylene emissions from the petrochemical industry.

摘要

近年來快速的城市化對局部範圍的大氣環流產生了深遠的影響，但對於控制對流層臭氧濃度的物理及化學反應機制仍然沒有完整的解釋。台灣由於嚴格的排放政策，相較於 1994 年，現今氮氧化物 (NO_x) 和揮發性有機化合物 (VOC_5) 的環境濃度已減少將近 60%。然而，減少這些前驅物並未使臭氧的年均濃度呈現線性的變化，在過去的十年間反而出現增加或趨於平緩的趨勢。因此，必須廣泛調查城市對於對流層臭氧化學的影響，以制定有效減少臭氧排放的方針。本研究針對台灣南部地區，其為一個由沿海城市、工業園區和內陸山區所組成的複雜區域，並經常於換季的時候 (4-5 月及 10-11 月) 發生高臭氧事件。在本篇論文中，吾人將使用城市規模解析度 1.0×1.0 公里的 WRF-CMAQ 模式，模擬臭氧及其前驅物 (如： NO_x 、 VOC_5) 的時空分布。

首先，吾人調查城市地表和當地環流的相互作用對當地氣候和臭氧空氣品質造成的影響。並對使用相同排放源但不同的特定地區進行了兩次模擬：城市情形代表當前城市化的現況；非城市情形則用農田取代所有城市網格。結果顯示，當城市熱島 (UHI) 氣流匯聚並停滯在城市上空時，會形成環流並將污染物困在較高的高度，並發現在 1000-1500 公尺的高空，羥基自由基與 VOC 的反應增加 $2.0\text{-}2.4 \text{ ppbv h}^{-1}$ 。在夜間，城市情形因為較深的邊界層使 NO_x 混合比稀釋了 17 ppbv，同時也削弱滴定效應，導致市區臭氧濃度升高了 15 ppbv。當 UHI 垂直混合減弱時，臭氧會從高空向下擴散至地表並進一步降低夜間空氣品質。

再者，吾人針對台灣南部城市及內陸地區邊界層內的 O_3 、 NO_x 和 NMHC 進行收支調查。在近地表的收支中，化學過程和乾沉降是使 O_3 匯入的主要原因，並且分別貢獻 10 ppbv h^{-1} 和 15 ppbv h^{-1} 以上；近地表的 O_3 垂直擴散超過 30 ppbv h^{-1} 。在邊界層收支中，化學過程是 O_3 主要來源，而垂直擴散也會使 O_3 匯入。物理化學牽涉近地表污染物的垂直擴散並增強 PBL 層上層的光化學反應來產生 O_3 ，並佔據城市中 O_3 的主要地位。這種垂直交換的過程主要是因為大氣能夠垂直擴散的結果，並隨高度增加逐漸地減弱交換效率。本研究結果發現白天的海風環流會將城市中受污染的氣團推向內陸，並且因為 NO_x 的限制條件，大大增強了內陸臭氧的生成，因此即使控制內陸地區的 NO_x 排放，也會受海陸風影響而沒有成效，然而大部分的城市地區，由於 VOC 的限制條件，控制 VOC 排放有助於降低 O_3 的排放。

最後，吾人基於 CMAQ-PMF 開發一個綜合指數，用來確認 VOC 的來源種類對於減少臭氧生成的貢獻性。利用 CMAQ-Higher Direct Decouple Method (HDDM) 確認研究區域的臭氧濃度對全域 (即城市、郊區和農村) 所排放之 NO_x 和 VOC 的一階、二階交叉敏感性 (cross sensitivities)。並發現南台灣城市地區 (內陸地區) 的臭氧生成敏感度因子，主要受在 VOC 限制條件 (NO_x 限制條件下)

下的 NO_x 負一階敏感度主導。大部分城市地區表明負 O₃ 凸反應曲線對 NO_x 排放表現出負二階敏感度，其中 NO_x 因排放很大程度上被非線性效應減弱而使 O₃ 線性增加。由於嚴格的 VOC 限制政策和減少或增加 NO_x 排放對生成 O₃ 相對地不敏感，本研究追求對臭氧形成最大貢獻 VOC 種類。VOC 使用 PMF 分析並解決八個因素，包括混合工業 (21%)、車輛排放 (22%)、溶劑使用 (17%)、生物源 (12%)、塑膠工業 (10%)、老化氣團 (7%)、機車尾氣 (7%) 和製造業 (5%)。研究結果顯示基於 CMAQ-PMF 的綜合指數，VOC 的控制措施應優先考慮以下排放源：(1) 油漆、塗料及印刷業對容易的使用，會排放大量的甲苯和二甲苯；(2) 汽油車所排放的 n-丁烷、異戊烷、異丁烷和 n-戊烷；(3) 石化業排放的乙烯及丙烯。



UMS
UNIVERSITI MALAYSIA SABAH

Acknowledgements

I would like to express my sincere appreciation and thanks to my advisor Professor Dr. Neng-Huei Lin, who have supervised my work and enormously helped me in many ways during my Ph.D. years in National Central University, Taiwan. Your insightful feedback encouraged me to sharpen my thinking and bring my work to higher level of excellence. To Dr. Stephen M. Griffith, I would like to thank you for your invaluable suggestions and efforts to improve, edit and critically review my work.

Many thanks to Dr. Maggie Chel-Gee Ooi, Dr. Steven Soon-Kai Kong, Dr. Wei-Syun Huang for providing excellent computing and technical support in model simulation, pre-processing reanalysis datasets and post-processing data visualization. I am also grateful to all research fellows, postdoctoral fellows, research associates and lab members from Cloud & Aerosol Laboratory (CAL) for their guidance and help throughout my study years in Taiwan.

I received Elite Scholarship from the Ministry of Education, Taiwan for the first three years of my graduate study. Additional financial support from my advisor and the National Central University for my fourth year.

Finally, I cannot end without thanking my late father, William Chang, my mother, Lily Chin and siblings, Watson Chang, Serene Chang & Nelson Chang for their absolute support that allowed me to advance further throughout my life. And to my special friend, Tan King Hong who always supported me and made me a better person in life.

CONTENT

Abstract	i
Abstract (Chinese)	iii
Acknowledgment	iv
Content	v
List of Figures	viii
List of Tables	xiii

Chapter 1: Introduction

1.1 Background Study.....	1
1.2 Problem Statement	3
1.3 Proposed Workflow	5
1.4 Objective.....	7
1.5 Scope	7

Chapter 2: Literature Review

2.1 WRF Urban Canopy Model	8
2.2 Bulk Urban Parameterization	10
2.3 Single-layer Urban Canopy Model	11
2.3.1 Solar fluxes.....	12
2.3.2 Longwave fluxes	13
2.3.3 Sensible heat flux	14
2.3.4 Wind speed in the canyon	15
2.3.5 Surface temperature.....	16
2.4 Multi-layer Urban Canopy Model.....	17
2.4.1 Momentum	18
2.4.2 Temperature	19
2.4.3 Turbulent kinetic energy	20
2.5 CMAQ Carbon Bond Mechanism	20
2.6 Impact of Urban Land-Surface Forcing on Ozone Pollution	23
2.6.1 Interaction between urban heat island (UHI) and local circulations	25
2.7 Budget Analysis of Ozone, NO _x , VOC	28

2.7.1 North & South America.....	28
2.7.2 Asia.....	30

Chapter 3: Impacts of land-surface forcing on local meteorology and ozone concentrations in a heavily industrialized coastal urban area

3.1 Introduction.....	37
3.2 Method.....	40
3.2.1 Study area.....	40
3.2.2 Episode description	41
3.2.3 Meteorology modelling system.....	41
3.2.4 Air quality modelling system	43
3.2.5 Experimental design	45
3.3 Result & Discussion.....	45
3.3.1 Model evaluation.....	45
3.3.2 Impacts of urban land-surface forcing on local meteorology.....	48
3.3.3 Impacts of urban modified boundary-layer on air quality.....	51
3.3.4 Interaction of urban-breeze and land-sea breeze on ozone air quality	54
3.3.5 Process analysis	61
3.3.6 Implications	66
3.4 Conclusion	68

Chapter 4: Process analysis of boundary-layer O₃, NO_x and NMHC in southern Taiwan

4.1 Introduction.....	70
4.2 Method.....	73
4.2.1 WRF-CMAQ model configuration	73
4.2.2 Gridded anthropogenic and biogenic emission	75
4.2.3 Urban canopy approach	77
4.2.4 Model evaluation.....	79
4.3 Results & Discussions	80
4.3.1 General description of local photochemical pollution.....	80
4.3.2 Near-surface ozone budget analysis	84
4.3.3 Boundary-layer budget analysis: O ₃ , NO _x and NMHC.....	87
4.3.4 Ozone production regime	102
4.3.5 Implications	109

4.4 Conclusion	112
----------------------	-----

Chapter 5: Development of a CMAQ-PMF-based composite index for prescribing an effective ozone abatement strategy: A case study of sensitivity of surface ozone to precursor VOC species in southern Taiwan

5.1 Introduction.....	115
5.2 Method.....	118
5.2.1 Study period & area.....	118
5.2.2 WRF-CMAQ model configuration	119
5.2.3 Higher-order decoupled direct method (HDDM).....	122
5.2.4 Positive matrix factorization (PMF) model.....	125
5.3 Results & Discussion.....	130
5.3.1 Decomposition of ozone response.....	130
5.3.2 Taylor-series expansion approximation.....	133
5.3.3 Sensitivity of individual modeled VOC species	137
5.3.4 Descriptive statistics of PAMS-VOC data & PMF optimal solution	144
5.3.5 Dominant sources of highly sensitive VOC species.....	148
5.4 Conclusion	153

Chapter 6: Summary

6.1 Key contributions.....	155
6.2 Future works.....	157

Appendix A: Supplementary Materials Chapter 3	158
---	-----

Appendix B: Supplementary Materials Chapter 4.....	179
--	-----

Appendix C: Supplementary Materials Chapter 5.....	186
--	-----

Bibliography	207
---------------------------	------------

List of Figures

Figure 1.1: Proposed workflow and thesis structure.....	6
Figure 2.1: Energy fluxes and temperatures for the three urban canopy models (UCM): (a) Single-layer UCM, (b) Multi-layer UCM, and (c) Slab model (Kusaka et al., 2001).....	9
Figure.2.2: The direct solar radiation (SD) incident on a horizontal surface. w is the normalized road width; h is the normalized building height ($w + r = 1$). Here r is the normalized roof width. I_{shadow} is the normalized shadow length on the road θ_z is solar zenith angle (Kusaka et al., 2001).....	12
Figure 2.3: Schematic diagram of the single-layer urban canopy model (SLUCM) and multi-layer BEP models (Chen et al., 2011)	17
Figure 2.4: Conceptual model of the processes prior to and after the development of a sea breeze propagating landward and how it impacts surface O_3 concentrations. In these sea breeze cases the surface temperature over the land in the morning is approximately equal to or less than the surface temperature over the water. Owing to daytime heating, the surface temperature over the land becomes greater than the surface temperature over the water in the afternoon (Martins et al., 2012)	26
Figure 2.5: Schematic diagram showing the vertical circulation of O_3 and its precursors in the boundary layer. (Tang et al., 2017).....	32
Figure 2.6: A schematic diagram of the regional O_3 transport mechanism proposed in Hu et al. (2018). .	33
Figure 2.7: Schematic diagram of the relationship between meteorological factors and O_3 production sensitivity. VOC: volatile organic compounds. (Zhao et al., 2019).....	34
Figure 2.8: Responses of air pollution control policies on ozone pollution in Beijing from 2013 to 2019. (Tang et al., 2021)	35
Figure 3.1: (a) Domain configuration (D01-D04) of the WRF-CMAQ model simulation with terrain height (shaded). (b) Land use/land cover (LULC) of D04. (c) NO and (d) isoprene emission rates averaged over the entire simulation period in the innermost domain D04	42
Figure 3.2: (a) Diurnal variation of observed and simulated O_3 concentrations averaged over the entire simulation period at urban stations ($n=10$) and rural stations ($n=5$). (b) Scatter plot of observed and simulated O_3 concentration over the entire simulation period separated for urban and rural stations. Red line represents 1:1 regression line. The IOA is index of agreement, MNB and MNE refer to the mean normalized bias and mean normalized error in unit percentage %. Color dots represent the density of the data where yellow indicates higher density of data and blue indicates the otherwise.....	46

Figure 3.3: Spatial distribution of O_3 (a,b) and NO_2 (c,d) concentrations (ppbv) overlaid with horizontal winds at the lowest model layer at 00 LST and 12 LST 10 Oct 2014. The color-filled circles represent the observed O_3 and NO_2 concentration overlaid on the simulation result. 48

Figure 3.4: Diurnal cycle of (a) surface air temperature and (b) planetary boundary layer height (PBLH) averaged over the urban area during the entire simulation period in the URBAN (E1_urban) and NO-URBAN (E2_nurb) scenario..... 50

Figure 3.5: Diurnal cycle of (a) O_3 , (b) NO_x , (c) O_x ($O_3 + NO_2$) and (d) CO concentration averaged over the urban area (refer Figure 3.6 for location of urban grid cells) at the lowest model level $n = 0$ ($h = 38m$) during the entire simulation period in the URBAN (E1_urban) and NO-URBAN (E2_nurb) scenario 52

Figure 3.6: Differences in O_3 concentration and horizontal wind field between URBAN and NO-URBAN simulation (E1 minus E2) in (a) daytime at 12:00 LST and (c) nighttime at 20:00 LST averaged during the entire simulation period. (b,d) Same as (a,c) but for NO_x concentration. All urban grid cells are highlighted by magenta dots..... 53

Figure 3.7: Vertical cross sections of (a) NO_2 concentration, (c) total advection process contribution to NO_2 concentration, (e) chemical process contribution to O_3 concentration, and the wind along the cross section A-B in Fig S3.8 at 12:00 LST averaged during the entire simulation period in the URBAN simulation. (b, d, f) same as (a, c, e) but for NO-URBAN simulation. 56

Figure 3.8: Vertical cross sections of total diffuse process contribution to O_3 concentration and the wind along the cross section A-B in Fig S3.8 at 12:00 LST (a) and 13:00 LST (c) averaged during the entire simulation period in the URBAN simulation. (b, d) same as (a, c) but for NO-URBAN simulation. 58

Figure 3.9: Vertical cross sections of (a) OH chain length, (c) rate of reactions between OH and VOC, (e) NO_2 production from the reactions between NO and peroxy radicals (HO_2 and RO_2), and wind along the cross section line at 13:00 LST in the URBAN simulation averaged during the entire simulation. (b, d, f) are the same as (a, c, e) but for the NO-URBAN simulation. 60

Figure 3.10: 4-h integrated vertical profiles of O_3 and the individual process contributions in (a, b) daytime and (c, d) nighttime separated for URBAN (solid line) and NO-URBAN (dotted line). All results are averaged over all the urban grid cells in domain D04 for the period from 11:00 to 14:00 LST for daytime and 19:00 to 22:00 LST for nighttime during the entire simulation period 62

Figure 3.11: Atmospheric boundary layer-averaged O_3 process contribution over the urban area during the entire simulation period in URBAN and NO-URBAN for daytime 11:00 to 14:00 LST (D) and nighttime 19:00 to 22:00 (N) 66

Figure 4.1: (a, b) Topography, domain settings, and monthly averaged emission over southern Taiwan. Anthropogenic source emission of (c) NO _x , (d) VOC are obtained from TEDS-10 emission inventory which has the base year 2016. The location of each TEPA air quality stations used in the current study are displayed on the innermost domain; red stars denote the Kaohsiung City stations, blue stars for Kaohsiung County Stations and green stars for Pingtung County Stations; details of each station is given in Table S3.3.	76
Figure 4.2: USGS land use category in domain (a) D03 and (b) D04. Urban class is further classified into three additional urban classes namely Low-Density Residential (31), High-Density Residential (32) and Industrial/Commercial (33) for single-layer urban canopy (UCM) scheme implementation.	77
Figure 4.3: Urban fraction (UF) distribution in the (a) default urban parameterization by look-up table and improved 2-Dimensional (2D) distribution using MODIS NDVI value in Domain (b) D3 and (c) D4.....	79
Figure 4.4: Distribution of (a) NO _x , (b) NMHC, (c) O ₃ , (d) O _x averaged during the entire simulation period at the lowest model level over southern Taiwan. Color contours are air pollutant concentration in ppbv and vector fields are horizontal UV wind at 10 m above ground.	83
Figure 4.5: Distribution of the contributions from (a) chemical process CHEM, (b) dry deposition DDEP, (c) vertical diffusion VDIF, (d) horizontal advection HADV to the near-surface O ₃ at the lowest model level (n=0) averaged during the entire simulation in Oct 2018. Wind fields represent the horizontal UV-wind vector at 10 m referenced at 5 m s ⁻¹ . Other less important contributions such as vertical advection ZADV, horizontal diffusion HDIF and cloud processes CLDS are shown in the supplementary material.	86
Figure 4.6: Spatial distribution of (a) CHEM, (b) VDIF, (c) HADV, (d) ZADV process contribution to O ₃ in the boundary layer (n=0 to n=9) averaged at 09-15 LST during the entire simulation period. Other less important process contribution DDEP, CLDS, and HDIF are provided in the supplementary material.	89
Figure 4.7: Spatial distribution of (a, b) EMIS, (c, d) HADV, (e, f) VDIF process contribution to NO _x and NMHC, respectively in the boundary layer (n=0 to n=9) averaged at 09-15 LST during the entire simulation period. Other less important process contribution CHEM, DDEP, HDIF and CLDS are provided in the supplementary material.....	92
Figure 4.8: Diurnal profile of the budget analysis in the boundary layer averaged over urban area (left panel) and inland area (right panel) for O ₃ , NO _x , NMHC during the entire simulation period in Oct 2018. Note that CLDS process in ozone budget is replaced by EMIS process in NO _x and NMHC budget which is more important in precursor budget analysis	95

Figure 4.9: Vertical profile of the budget analysis in the boundary layer averaged from 09 to 15 LST over urban area (left panel) and inland area (right panel) for O₃, NO_x, NMHC during the entire simulation period. Red and blue marked line represents the concentration at 09 LST and 15 LST, respectively. The tick mark on bottom x-axis beyond ±40 is scaled to ±100, ±200, ±300 and ±400 to facilitate comparison. Note that CLDS process in ozone budget is replaced by EMIS process in NO_x and NMHC budget..... 101

Figure 4.10: Spatial distribution of OMI and CMAQ O₃ sensitivity regime using the ratio VCD HCHO/VCD NO₂ and P(H₂O₂)/P(HNO₃), respectively. Ratio HCHO/NO₂ in VCD greater than 4.2 represents NO_x-limited regime, in between 2.3 and 4.2 represents transition regime, and lower than 2.3 represents VOC-limited regime. Ratio P(H₂O₂)/P(HNO₃) greater than 0.2 represents NO_x-limited regime, in between 0.06 and 0.2 represents transition regime, and lower than 0.06 represents VOC-limited regime 103

Figure 4.11: Spatial distribution of P(H₂O₂)/P(HNO₃) ratio at 09 LST and 15 LST averaged during the entire simulation period at the model layer n = 0 and n = 5..... 106

Figure 4.12: Spatial distribution of OH chain length at 09 LST and 15 LST averaged during the entire simulation period at the model layer n = 0 and n = 5..... 107

Figure 4.13: (a, b) Classification of ozone production sensitivity regime using P(H₂O₂)/P(HNO₃) averaged from 09-15 LST at model level n = 0 and n = 5. All urban grid cells are represented by black dots overlaid on the map. (c, d) Vertical profile of O₃ at 09 LST (red marked line) and 15 LST (blue marked line) and its process contribution averaged from 09-15 LST over all urban grid cells classified as VOC-limited regime and NO_x-limited regime respectively 110

Figure 5.1: (a) Domain configuration of four-nested grid system, (b) land use of the innermost domain, (c, d) monthly averaged NO_x and VOC emissions in the innermost domain obtained from 2016 TEDS-10 emission inventory. The location of each TEPA air quality stations (red stars) and PAMS stations (red dots with label) used in the current study are displayed in the innermost domain. Refer Figure S3.2 and Table S3.3 for details of each TEPA and PAMS station..... 120

Figure 5.2: Overall framework of the Positive Matrix Factorization (PMF) model methodology. Processes in the dashed-line box are repeated for 3-8 factor number combinations. MDL: minimum detection limit 127

Figure 5.3: CMAQ-HDDM first-order sensitivity coefficient of O₃ to (a) NO_x emissions, (b) VOC emissions, second-order sensitivity coefficient of O₃ to (c) NO_x emissions, (d) VOC emissions, (e) second-order cross sensitivity coefficients of O₃ to NO_x, VOC emissions, at daytime 09-15 LST averaged during the entire simulation period. Magenta and green highlighted borderline represents Xiaogang district and Pingtung region, respectively..... 131

Figure 5.4: Spatial distribution of O_3 concentration in (a) baseline with no perturbations in NO_x and VOC emissions, and changes in O_3 concentration under (b) NO_x control scenario, (c) VOC control scenario, and (d) NO_x & VOC control scenario at daytime 12 LST. All scenarios reduced the targeted emissions by 5% except for the baseline..... 135

Figure 5.5: Taylor-series approximation of ∂O_3 against ∂VOC emissions at different level of projected ∂NO_x emissions for (a) Xiaogang (urban) and (b) Chaozhou (inland) averaged at 12:00 LST. Projected ∂NO_x emissions at 0% (black line) and -5% (red line) represents the current year 2018 and near future 2025, respectively; other projected ∂NO_x emissions at arbitrary -50%, $\pm 25\%$ are presented for far-future comparison purpose 137

Figure 5.6: (a) Daily averaged CMAQ-DDM first-order sensitivity coefficient of O_3 concentrations calculated per number of grids to each modelled VOC species arranged in ascending order for urban and inland area. Sensitivity of O_3 and ozone formation potential (OFP) to (b,e) alkenes emissions (OLE + ETH + IOL), (c,f) aromatics emissions (XYL + TOL), and (d,g) alkanes emissions (PAR) at 12 LST..... 140

Figure 5.7: Diurnal variations of the CMAQ-DDM sensitivity of O_3 to the six most sensitive VOC modelled species (i.e. terminal olefins, OLE; xylene, XYL; paraffin, PAR; ethene, ETH; toluene; TOL; internal olefins, IOL) averaged for (a) urban and (b) inland area, during the entire simulation period..... 141

Figure 5.8: Relative distribution in percentage of (a) CMAQ DDM O_3 sensitivity and (b) CMAQ EMIS hydrocarbon emissions to individual VOC summed across different groups averaged for urban and inland area during the entire simulation period..... 143

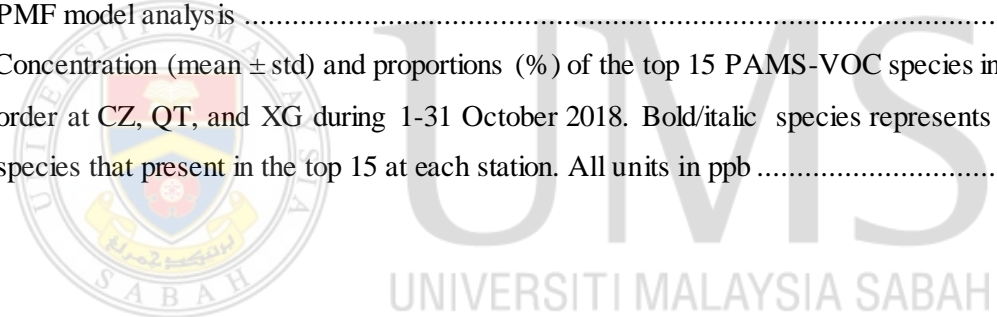
Figure 5.9: Source profiles calculated using the PMF model at Chaozhou, Qiaotou, Xiaogang PAMS stations 147

Figure 5.10: Diurnal variations of factor contribution calculated by the PMF model at Chaozhou, Qiaotou, Xiaogang PAMS stations 148

Figure 5.11: Normalized factor contribution and composite index of source profile to each PAMS-VOC species at Chaozhou, Qiaotou, Xiaogang PAMS station 152

List of Tables

Table 2.1 Overview of carbon bond mechanism CB-IV, CB05, and CB6.....	21
Table 5.1 Perturbed emissions considered in the 25 sensitivity tests. The first 5 sensitivity tests S1-S5 accounts for the first-order, second-order and cross-order sensitivity due to the domain-wide NO _x and VOC emissions and the other 20 sensitivity tests S6-S25 accounts for the individual VOC model species.....	124
Table 5.2: Categorization of PAMS-VOC species for PMF model source apportionment analysis. Grey-highlighted species represents unused species with abundant missing data >55% below minimum detection limit (MDL). Poor category species are identified for low S/N <0.5. Weak (Strong) category species are identified for S/N ≥0.5 and R ² <0.6 (R ² ≥0.6) between measured and modelled concentration predicted by PMF model. Both unused and bad species are removed from PMF model analysis	128
Table 5.3 Concentration (mean ± std) and proportions (%) of the top 15 PAMS-VOC species in ascending order at CZ, QT, and XG during 1-31 October 2018. Bold/italic species represents the unique species that present in the top 15 at each station. All units in ppb	145



Chapter 1 Introduction

1.1 Background Study

In recent years, southern Taiwan has been facing severe ozone air quality pollution, particularly during the seasonal transition period under the weak synoptic weather condition. Due to the strengthened emission control policy, the mean PM_{2.5} concentrations has significantly declined in the last decade but the ozone concentration did not follow the similar declining trend and rather an increasing or flattening trend, reflecting a greater urgency for ozone pollution abatement. [Chou et al. \(2006\)](#) showed that the ozone concentration in Taipei, Taiwan increased substantially during 1994-2003 despite its precursors nitrogen oxides (NO_x) and non-methane hydrocarbon (NMHC) decreased significantly in the same period. The annual average of ozone and daily maxima ozone increased by 58% and 26% respectively in Taipei from 1994 to 2003. [Chang et al. \(2017\)](#) also reported that ozone concentration in Taiwan continued to increase from 2000 to 2014 with the increasing rate of daily 8h maxima (+0.45 ppb yr⁻¹) is more than twice as great as the daytime average (+0.20 ppb yr⁻¹). A more recent study from [Tsai and Lin \(2021\)](#) showed that despite all pollutants (i.e. PM, SO₂, CO, NO₂) in Taiwan has a consistent declining trend from 2014 to 2020, annual average ozone has an increasing trend fluctuating in the range 54-60 ppb. Considering that near-surface ozone is greenhouse gases and harmful to human health ([Yim et al., 2019](#)), crop ([Avnery et al., 2011](#); [Tai and Val Martin, 2017](#)) and ecosystem ([Ashmore, 2005](#)), it is essential to examine the possible reasons related to the increasing trend of ozone concentration both regionally and locally.

Tropospheric ozone is closely related to its precursors NO_x and NMHC emissions both anthropogenic and biogenic. It is a major secondary air pollutant, produced through a complex series of photochemical reactions involving NO_x and NMHC. High O₃ episodes are usually associated with hot sunny weather, low wind speed stagnant condition, and slow-moving high pressure system. The consequences of these systems can influence the long-lived pollutants such as NO_x, NMHC and CO in terms of spatial transport ([Lu et al.,](#)

2019), accumulation and kinetic reaction (Chen et al., 2020), which are directly related to the ozone formation. The ozone production regime is characterized by its sensitivity production either VOC-limited or NO_x-limited. The split between NO_x-limited or VOC-limited regime is determined by the chemistry of odd hydrogen radicals of either peroxides (i.e. hydrogen peroxide (H₂O₂), organic peroxides (ROOH)) or nitric acid (HNO₃). When the peroxides are the dominant radical sinks, the ozone chemistry favors NO_x-limited regime; when the nitric acid is the dominant sink, VOC-limited regime is favored. It is crucial to identify the ozone production regime for effective ozone pollution control measures because reducing NO_x emission in VOC-limited regime could have the adverse effect of increasing the O₃ concentration, while reducing VOC emission in NO_x-limited regime has little to insignificant impact on O₃ concentration.

Urbanization is an irreversible process involves the change of land use land cover from natural surfaces to artificial impervious surfaces. One of the most well-known impacts of urbanization is urban heat island (UHI) effect. UHI is characterized by a strong temperature gradient between the urban core and its surrounding areas generating a convergent flow towards the urban center in the lower boundary layer and a divergent flow from the upper boundary to the urban outskirts (hereinafter referred as urban-breeze) (Oke, 1976; Saitoh et al., 1996). At local scale, weather condition such as high temperature and low wind speed are conducive to UHI development and can induce a persistent convergence favorable to ozone formation in the urban areas (Martinelli et al., 2020; Umezaki et al., 2020; Yoshikado and Tsuchida, 1996). For coastal city, the interaction of UHI with local circulations (i.e. land-sea breeze) further complicates the ozone and its precursors transport through complex recirculation patterns (Finardi et al., 2018). During the daytime when entrainment process is unfolded, ozone is injected into the rapidly growing boundary layer. The drop in boundary layer depth that occurred when sea breeze front moved inland, carrying polluted urban air of NO_x-rich air and facilitated near-surface ozone titration effect, also had an impact on the vertical ozone profile. During the nighttime when the land-breeze is prevalent, the advected urban polluted air mass is transported back to the urban area.

To mitigate the ozone pollution problem, several attempts are suggested and extensively reviewed in the literatures. These methods can be grouped into two categories: (1) passive control and (2) active control. Passive control of ozone is usually done by reducing the UHI effect to reduce the ozone formation rate meanwhile active control is related emission control that targeted on the ozone precursors such as NO_x and NMHC. In the passive control, [Fallmann et al. \(2016\)](#) evaluated the effectiveness of urban greening and highly reflective material roof (i.e. white roofs) on the ozone concentration inside the urban canopy layer and found that both urban greening and white roofs are able to reduce the urban temperature by about 1 K and the mean ozone concentration by 5-8%. Other passive control strategies include installing green roofs ([Li et al., 2014](#)) or using permeable material pavements for highly populated cities, and proposing effective mitigation strategies based on sea breeze patterns ([Sasaki et al., 2018](#)). In the active control, it is important to first identify the ozone sensitivity production regime of the area of interest. For instance, [Chang et al. \(2016\)](#) concluded that the controls of NO_x emissions would mitigate ozone air pollution in most of the suburban cities in United States due to the NO_x -limited condition but control of VOC emissions is more effective to curb ozone air pollution in highly populated cities of VOC-limited condition. In another study, [Tang et al. \(2017\)](#) reported that the implementation of emission control during the Beijing Olympics 2018 decreased the ozone precursors (i.e. NO_x and NMHC) throughout the boundary layer but elevated the ozone concentration in the central urban area by more than 8 ppb. This is likely due to the weakened titration effect stems from the reduced NO_x emission especially for area of highly VOC-limited condition. The study also highlighted the temporary Beijing Olympics 2018 emission control measures expanded the region controlled by both NO_x and VOC and decreased region controlled by VOC.

1.2 Problem Statement

Tropospheric ozone is a secondary pollutant formed when the nitrogen oxides (NO_x) and volatile organic compound (VOCs) react in the atmosphere in the presence of sunlight. While ozone in the stratosphere is useful to protect the planet's surface from the harmful ultraviolet radiation, but ozone in the troposphere or ground-level ozone is the main component of photochemical smog. When present in high concentration, it

can cause adverse respiratory effects such as difficulty to breathe, increased susceptible to respiratory diseases, increased sensitivity to allergens (Karthik L et al., 2017), and long term exposure may result in permanent lung damage (Zhang et al., 2019). Ozone is also a plant toxic when enforced by the presence of SO₂ and NO_x can reduce the crop yields (Avnery et al., 2011; Tai and Val Martin, 2017), damage agricultural crops, forests and wilderness areas (Ashmore, 2005).

Over the past several decades, rapid urbanization with increased anthropogenic emissions have substantially increased the adverse effect of UHI as well as the local air quality (Ohara et al., 2007). The UHI effects on air quality stem from the impacts of urbanization on local meteorology. Local studies in Taiwan show that UHI can enhance the daytime sea-breeze and weaken the nighttime land-breeze and thus had a significant impact on the air pollution dispersion in Taiwan (Lin et al., 2008). Besides, UHI effects also play an important role in perturbing thermal and dynamic processes; the convergence system induced by UHI prevented water vapor from being transported by the sea-breeze to the mountainous area and thus delay thunderstorm development (Lin et al., 2011). Since the 1990s, ozone has shown an increasing trend and has become the main air pollutant in southern Taiwan (Chang et al., 2005) which is located in the western coastal region where local circulation is prevalent under weak synoptic weather condition. Kaohsiung city located in southern Taiwan hosted many heavy industries such as petrochemical, refinery, steel-making, and power generation plants. It is also the second largest city in Taiwan which is densely populated approximately 2.7 million inhabitants. The coastal area of Kaohsiung City has the worst air quality in Taiwan because to the several industrial parks that are scattered around the city. Three main power plants are also located within 35 km of the city. The impact of urbanization on local meteorology such as urban heat island effect is well documented in the literatures but very few studies extended to air quality investigations. Ambiguity on the interaction between the UHI effect and local circulations (i.e. land-sea breeze) as well as its possible impacts on ozone air quality remains poorly established.

Due to the stringent emission control policies implemented in the recent years, a decline in NO_x emission by -23% was estimated in Taiwan from 2010 to 2016 using Ozone Monitoring Instrument (OMI) tropospheric nitrogen dioxide (NO_2) retrievals during the Korea-United States Air Quality (KORUS-AQ) campaign over East Asia (Souri et al., 2020). The study also highlighted that Taiwan stand out as region experiencing lower MDA8 ozone levels due to the continuous NO_x reductions throughout the years, especially for areas primarily in NO_x -sensitive condition. Changes in NO_x and VOC emission could lead to increase or decrease in O_3 concentrations depending on the O_3 sensitivity regime. In addition, the local circulation and urban land-surface forcing further complicates the non-linearity of the complex reaction between O_3 - NO_x -VOC, making the mitigation policy becomes difficult at urban scale. To reduce the severe photochemical pollution in southern Taiwan, control techniques are required due to the increasing atmospheric oxidation capacity brought on by ongoing urbanization. The large gap in the O_3 budget studies over southern Taiwan may result in the implementation of unsuitable policy. Our knowledge of the budget analysis of the O_3 and its precursors in the vertical profile still has many gaps and uncertainties, which results in a lack of precision in the O_3 pollution reduction strategy across southern Taiwan.

1.3 Proposed Workflow

This thesis adopted the WRF-MEGAN-CMAQ model to simulate the spatial and temporal distribution of O_3 and its predecessors (i.e. NO_x , NMHC) over southern Taiwan at urban scale resolution 1.0 km x 1.0 km. The urbanization in the model is invoked by implementing the single-layer urban canopy (SUCM) scheme in the modelling system. The accurate representation of the urban meteorology fields is crucial in the chemical transport modelling because the chemical production and physical transportation of air pollutants are closely linked with the meteorology at urban scale. Anthropogenic emission is provided by Model Inter-Comparison Study for Asia, MICS at the outer domain (i.e. East China) and Taiwan Emission Data System, TEDS at the inner domain (i.e. Taiwan). The emission inventory contains point, line and area sub-inventory sources which are further estimated into gridded and hourly emissions through the use of SMOKE model. Biogenic emission is provided by the MEGAN v2 model which is driven by the latest plant functional type